Journal of Materials Chemistry C

Accepted Manuscript

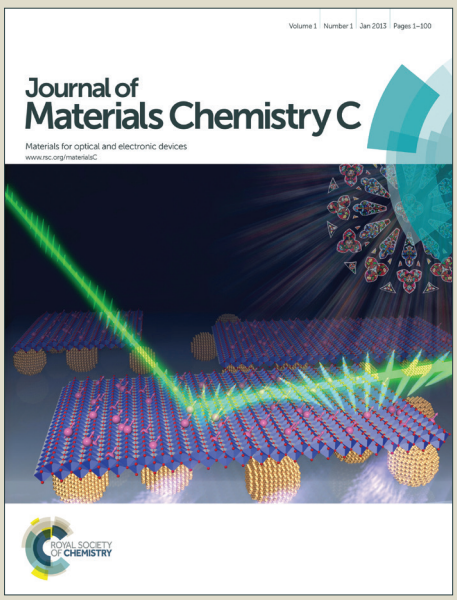

ROYAL SOCIETY OF CHEMISTRY

www.rsc.org/materialsC

Journal of
Materials Chemistry C

RSCPublishing

COMMUNICATION

Aligned gold nanobowl arrays: their fabrication, anisotropic optical response and optical grating application

Cite this: DOI: 10.1039/x0xx00000x

Received 00th January 2014,
Accepted 00th January 2014

DOI:

www.rsc.org/

Xinyang Li[a], Yanchun Wu[a], Lifeng Hang[a], Dandan Men[a,b], Weiping Cai[a], Yue Li[*a,b]

A simple, low-cost and high-throughput technique to fabricate aligned Au nanobowl arrays is presented combining template-assisted self-assembly and colloidal lithography. Polystyrene (PS) colloids were self-assembled into the aligned grooves on blank digital versatile disc (DVD) substrate, forming aligned PS colloidal necklace arrays. After coated an Au layer, they were inverted onto another glass slide with polyvinyl alcohol (PVA) thin layer and aligned Au nanobowl arrays were obtained after peeling off DVD substrate and removing the PS colloidal spheres. If the glass slide substrate was removed, the aligned Au nanobowl arrays on a flexible PVA substrate could be achieved. These Au nanobowl alignments displayed higher reflectance and could be used as optical grating. They also demonstrated anisotropic optical properties, which important potential applications in optical devices, such as optical grating, waveguide, and so on. This work will provide new insights and understanding on the control of morphology and enhancement of optical properties of Au nanoparticle arrays and it is helpful to develop new optical device based on such anisotropic optical performance.

1. Introduction

Periodic nanostructured arrays with units of finite sizes and shapes have attracted numerous attentions due to their applications in energy conversion and energy storage in the past several decades[1-3]. Particularly, noble metal nanostructured arrays are of major interest in the fields of nanophotonics, optical sensing, and other advanced applications owing to their unique optical and biotechnological properties.[4-6] To take advantage of these special properties for future devices, techniques in precise control of nanostructured arrays need to be developed. The most widely used manufacture techniques are lithography techniques including photolithography, electron beam lithography, nanoimprint lithography, and focused ion beam lithography, etc.[7-11] They have abilities to create the nanostructured arrays with high quality, but the problems of high cost, low throughput and difficulty in accessing the facilities remain unsolved. Besides these conventional techniques, techniques based on self-assembling have proved to be promising, alternative strategy to prepare nanostructured arrays for the advantage in terms of low cost, reproducibility.[12,13] For instance, a self-assembled colloidal monolayer can be used as a template or mask to prepare periodic nanostructured arrays, including units of nanoparticle, nanopore or nanorod assisted by chemical and physical processes.[14-16]

Recently, aligned nanoparticle arrays with high aspect ratio were studied for its anisotropy in optical response. Research in optical anisotropy is of great importance in feedback laser, holography, etc. Particularly, metal nanoparticles growth on ripple-patterned substrate is a rather new approach to produce nanoparticle or nanowire arrays of desired periodicity.[17-20] Moreover, it was reported that the metal nanoparticles deposited on ripple pattern shows unique plasmonic and magnetic properties.[21-23] Oates et al. [20] found that ordered metal nanoparticle arrays on such ripple pattern substrate presented different local surface plasmon resonance (LSPR) modes along and across the ripples. Ranjan et al.[24,25] fabricated Ag nanoparticle arrays grown on ripple patterned templates by oblique incidence physical vapor deposition, and such periodic arrays demonstrated that anisotropic coupling of nanoparticles was responsible for observed optical anisotropy. Furthermore, it is well-known that size and shape of particles, and gap between particles have great effect on plasmonic properties.[26,27] However, physical vapor deposition growth makes Ag nanoparticles size ununiformed and not well aligned in arrays. From a technological point of view, the application of metal nanoparticles with plasmonic properties demands a fully controlled growth process. Therefore, it is an essential prerequisite for developing a high-efficient and time-

[a] *Key Laboratory of Materials Physics, Institute of Solid State Physics, Anhui Key Laboratory of Nanomaterials and Nanotechnology, Chinese Academy of Sciences, Hefei, 230031, Anhui, China*
[b] *University of Science and technology of China, Hefei 230026, P. R. China*
Tel: 0086-551-65595323, E-mail: yueli@issp.ac.cn

saving technique to fabricate aligned nanoparticle arrays for optical application.

The controlled synthesis of units of arrays with desired morphologies and architectures at micro- and nano-scale levels is crucial to tune LSPR. To date, most of the work has focused on the fabrication of symmetric metallic nanoparticles due to its wide applications.[28-30] Recently, it was reported that breaking the symmetry would result some extraordinary optical properties on symmetric nanoparticles by reason of its anisotropic morphology. Several sorts of reduced-symmetrical nanostructures have been fabricated these years, such as nanobowl,[31,32] nanocrescent,[33] nanohoneycomb,[34] and nanoring.[35,36] Particularly, reduced-symmetrical nanostructure of Au nanoparticles such as nanocup and nanocap, has a number of interesting consequences, owning to its tunable LSPR. These reduced-symmetrical nanostructure of Au not only showed highly tunable optical properties, but also rendered their optical properties dependent on the angle and polarization of the incident light.[37,38] To the best of our knowledge, very limited studies on Au nanobowl structures have been reported. For example, Ye et al. [39,40] developed a complex method involving an ion milling technique and a vapor HF etching process to fabricate upward Au nanobowl monolayer structures. The Au semishells exhibit enhanced absorption and scattering cross sections at higher wavelengths, compared to full Au nanoshells. However, the application of this fabrication technique is limited by their complicated fabrication steps. Therefore, much effort should be devoted to developing simple but effective techniques for fabricating nanostructured arrays consist with reduced-symmetrical units.

Herein, we report a simple, low-cost and high-throughtput technique combining template-assisted self-assembly and colloidal lithography to fabricate aligned Au nanobowl arrays. First, polystyrene (PS) colloids were orderly arranged into the aligned grooves on inexpensive, blank digital versatile disc (DVD) substrate by a simple template-assisted self-assembly technique. An Au layer was then deposited on these aligned PS colloidal necklaces filled in DVD grooves. And such PS colloidal necklaces with Au layer were inverted onto another substrate (glass slide) with polyvinyl alcohol (PVA) thin layer. After peeling off DVD substrate, PS spheres with Au caps were transferred onto another substrate. Finally, aligned Au nanobowl arrays were obtained by removing the PS colloidal spheres. Additionally， after the glass slide substrate was removed, the aligned Au nanobowl arrays on a flexible PVA substrate could be achieved. Such aligned Au nanobowl arrays displayed higher reflectance and could be used as optical grating. And they also demonstrated anisotropic optical properties. This work will provide new insights and understanding on the control of morphology and enhancement of optical properties of Au nanoparticles, and such aligned Au nanobowl arrays have important potential applications in optical devices, such as optical grating, waveguide, and so on.

2. Experiment

2.1 Materials.

Polystyrene (PS) spheres with 500 nm diameter in aqueous suspension (2.5 wt %) were purchased from Alfa Aesar Corporation. Deionized water (18.2 MΩ/cm) was obtained from an ultrafiltration system (Milli-Q, Millipore, Marlborough, MA). The blank Digital Versatile Discs (DVD) was purchased from Philips Corporation. All the reagents used in this research were analytically pure without further purification.

The DVD structure generally consists of two polycarbonate discs, with grooves spiraling from its center to its periphery on the scale of hundreds nanometers on the inner surface. So the inner surface of a DVD could be used as a template. A thin metallic film as a reflecting layer and a dye-containing layer as the recording medium were sandwiched between up and bottom discs. The two discs were mechanically separated, and samples of rectangular shape with length of several centimeters were cut from the periphery of the DVD. In this region, the grooves are of a width of *ca.* 300 nm, a depth of *ca.* 100 nm and a periodicity of *ca.* 800 nm. The DVD substrate with aligned grooves on surface was rinsed by ethanol to remove dye on the surface. After washed by ultra-sonication in deionized water, the substrate was dried followed by 10 min treatment in UV-ozone cleaner to make the surface hydrophilic to guarantee further self-assembly of PS spheres on their grooves.

2.2 Fabrication of aligned Au nanobowl array.

Figure 1 describes the fabricating process of aligned Au nanobowl arrays. First, PS spheres were self-assembled into the grooves of DVD substrate using fluidic cell（figure 1a）. Then a thin layer of Au (*ca.* 40 nm in thickness) was deposited on the PS colloidal sphere necklace array on the DVD substrate via plasma sputtering at a rate of 6 nm min^{-1} in thickness (figure 1b). The thickness of the Au layer could be controlled by adjusting the sputtering time when other conditions were fixed. A thin film (*ca.* 10 μm in thickness) of polyvinyl alcohol (PVA) was spin coated on a planar glass slide (another substrate). In succession, the aligned PS colloids array with a thin Au layer on a DVD substrate was inverted onto a PVA film with conformal contact under pressure of 0.2×10^5 Pa (figure 1c). After a few minutes, the DVD substrate was peeled off, leaving PS spheres with Au nanocaps at each sphere bottom on the PVA thin film (figure 1d). The PVA film with aligned PS spheres with Au nanocaps was immersed in methylene chloride (CH_2Cl_2) solution for several minutes to dissolve the PS spheres and aligned Au nanobowl arrays were finally achieved (figure 1e). In addition, the PVA film could be peeled off from glass slide, a flexible film with Au nanobowl linear array can be obtained (figure 1f).

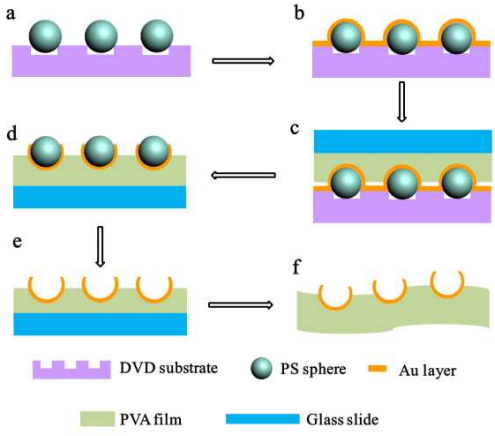

Fig. 1 Schematic illustration of the fabrication strategy of aligned Au nanobowl array. Each inset in this scheme represents the cross-section which is perpendicular to grooves on DVD substrate, and each PS sphere in scheme represents a chain of PS sphere in fact. (a) PS spheres' assembly on DVD grooves; (b) deposition of Au layer onto aligned PS spheres and DVD substrate; (c) glass slide with a thin layer of PVA get conformal contact with aligned PS spheres coated with Au layer; (d) aligned PS spheres with Au coatings around were transferred onto glass slide; (e) PS spheres were removed by dissolving in CH_2Cl_2 solution; (f) PVA film peeled off from glass slide.

To obtain aligned PS sphere arrays on the grooves of DVD substrate, a template-assisted self-assembly process was performed[41-43]. A template-assisted self-assembly process was carried out to obtain aligned PS sphere arrays on the grooves of DVD substrate. Firstly, a fluidic cell was fabricated. As shown in the figure 2a, fluidic cell was simply created by sandwiching a thin frame of Mylar film between two parallel substrates. It should be noted that the bottom substrate was DVD substrate with grooves upwards, while the top substrate was a glass slide with a small hole (*ca.* 2 mm in diameter) drilled on it, and then a glass tube was fixed to this hole with epoxy. Afterwards, this sandwiched structure was tightened with binder clips. Then, aqueous dispersion of PS spheres was injected into the fluidic cell through the glass tube. And the suspension was confined in the fluidic cell to make it flow slowly along the grooves. As a result, this aqueous suspension can continuously evaporate through the glass tube when it is flowing. Finally, the PS spheres can be self -assembled into the grooves on the DVD substrate when the liquid was dewetted from bottom surface of DVD substrate. As the meniscus slowly recedes across the substrate, PS spheres concentrate at the three-phase contact line. There were three major forces was exerted on each sphere during the process, which are capillary force associated with the meniscus of the liquid, gravitational force and electrostatic force caused by charges resting on the surfaces of the PS spheres and the substrate. Particularly, the capillary force that originates from the liquid meniscus plays the most important role in pushing PS spheres into the grooves on DVD substrate. Furthermore, the strength of the attraction capillary forces between adjacent spheres in the same groove is much larger than those between spheres in adjacent grooves, so all the spheres stayed in the grooves with certain orientation.

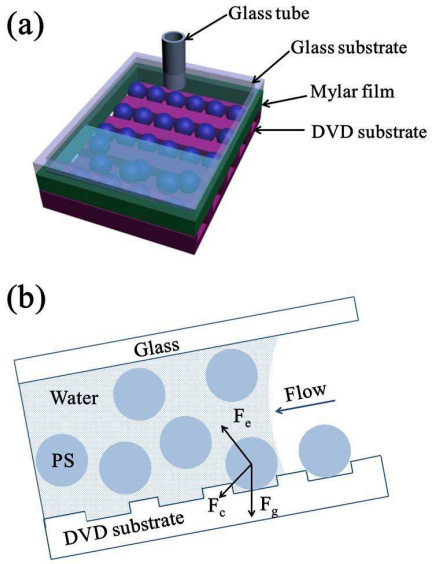

Fig. 2 (a) A schematic illustration of the fluidic cell that was used to assemble PS spheres into grooves on the DVD substrate. (b) A cross-sectional view of the fluidic cell. For a PS sphere next to the rear edge of the colloidal suspension, there are three possible forces exerted on it: the capillary force (F_c), the gravitational force (F_g), and the electrostatic force (F_e).

2.3 Characterization.

The morphology of samples was observed by a field-emission scanning electronic microscope (FESEM, sirion 200 FEG). Optical transmission and reflection measurements in different angle of incident light were carried out with Ideaoptics PG2000-Pro-Ex system equipped with a FIB-600-DUV optical fiber. The spectra integration time of collecting the signals was set to be 11 ms. A special support named R1 series (Ideaoptics instrument Co., LTD) with 360° rotating arms equipped with light source and detector respectively, and a horizontal sample stage in the center was also employed.

3. Results and discussion

3.1 Morphologies and structures

Figure 3 presents morphologies of the samples obtained in some certain steps. Figure 3a shows the typical FESEM image of blank DVD substrate with parallel aligned grooves (a groove width: *ca.* 300 nm, its depth: *ca.* 100 nm and its periodicity: *ca.* 800 nm). The PS spheres are arranged into grooves on substrate by template-assisted self-assembling process, forming a colloidal necklace alignment, as shown in figure 3b. All the PS spheres were self-assembled along the substrate grooves, yielding an array of parallel colloidal chains with a controlled preferential orientation. It is worth noting that there were little space between PS spheres in each chain, which may because of attraction capillary forces and repulsion electrostatic force between two spheres. Additionally, because the width of grooves was *ca.* 300 nm, and the depth was *ca.* 100 nm, so PS spheres with diameter from 300 nm to 500 nm would get stuck in the groove and only a string of PS spheres could be self-assembled into the groove according to geometrical configuration. A thin Au layer was deposited on aligned PS sphere chain array with its substrate via plasma sputtering. Such aligned PS sphere arrays with thin Au layer was transferred onto another glass slide which was spin coated with a thin film of PVA, as displayed figure 3c. One can find the aligned PS spheres coated with Au layer had been successfully transferred on the new substrate (glass slide) without obvious defects. It can be observed that spheres in one chain get closer to each other compared with ones before coating Au layer. This was attributed to Au coating on PS spheres, decreasing the interspace between neighboring spheres. The deposited Au layer on the substrate between grooves could not contact with PVA film during transferring process, this part of Au layer would be left on the DVD substrate when the substrate was separated from glass slide, so the aligned PS sphere array with Au layer at sphere bottom was remained. The aligned Au nanobowl chain is formed on substrate after removing PS spheres by chemical dissolution, as demonstrated in Figure 3d, 3e. As it was shown in figure 3d, Au nanobowl has open mouth on its top and it seems like a quasi-ellipsoid from top view. The long axis of the ellipsoid was about 500 nm, the same as diameter of PS sphere template; nonetheless, the short axis of that was 470 nm or so, a little smaller than diameter of PS sphere template. This phenomenon can be explained as follow: the direction parallel to the chains, there was a good adhesion between neighboring nanobowls due to deposited Au layer in preparing process. Therefore, the Au layer would not shrink much on this direction when one PS sphere was dissolved in CH_2Cl_2. On the other hand, for the direction perpendicular to the chains, there was no force to support the nanobowl wall, so the wall of nanobowl at top along short axis would shrink slightly to the center due to capillary force of solvent during solvent evaporation. In one word, Au nanobowls were upwards parallel aligned with certain orientation and Au nanobowls in one chain were conterminal. In addition, this PVA film can be peeled off from the glass slide, aligned Au nanobowl arrays on a flexible film can be obtained through this way. As can be seen in figure 3f, photograph of as prepared aligned Au

nanobowls on PVA film, the size of aligned Au nanobowl arrays fabricated by this process achieved several millimeters, which is perfect for further applications.

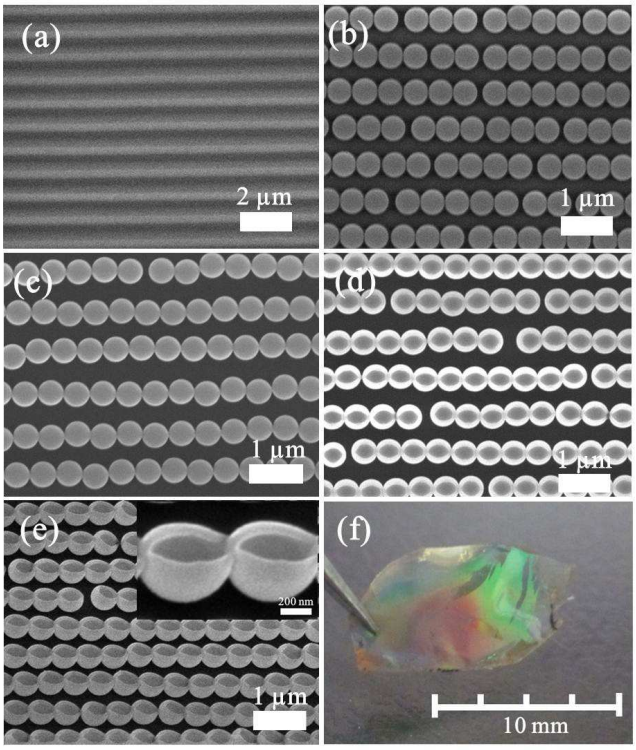

Fig. 3 The morphologies of the samples obtained in different steps: (a) typical FESEM image of blank DVD with aligned grooves on inner interface; (b) FESEM image of aligned PS sphere array on DVD grooves; (c) FESEM image of aligned PS sphere array in (b) transferred onto glass slide after deposition of Au layer; (d) and (e) top viewed and 45°-tilted FESEM image of aligned Au nanobowls. The inset in (e) is the local magnified image; (f) Photograph of as prepared aligned Au nanobowls on a flexible PVA film.

3.2 Optical transmission with anisotropy

This kind of nanostructured array with a high aspect ratio, periodicity and symmetry-reduced is likely to be sensitive to angle of incident light. Angle-resolved transmission measurements were performed at oblique incidence for the aligned Au nanobowl arrays on a flexible PVA film, as presented in figure 4. Figure 4a briefly illustrated the configuration of the angle-resolved measurements. At normal incidence the light beam makes angle α and β to be 0°. The angle of incident light relative to the sample surface was varied in two distinct ways: (1) the incident light was moving in the planar perpendicular to Au nanobowl chains, angle α changed from 0° to 30°, and the transmission light was detected underneath the sample with changing location corresponding to the incident light; (2) the incident light was moving in the planar parallel to Au nanobowl chains, angle β changed from 0° to 30°, other experimental setup was same with (1). In the process of measuring, the prepared sample was fixed horizontally, while light source and detector were rotated around simultaneously. And the spectra shown in figure 4c and d were recorded varying incidence angle of an interval of 2° for each measurement. A halogen lamp (wavelength from 400 nm to 1100 nm) was used as light source.

The transmission spectra with changes of incidence angle were shown in figure 4b and c. One can see that transmittance intensity decreased with increasing incident angle (α or β) due to a reduce in the in-plane component of incident light wavevector perpendicular to the PVA film when α or β increased. The transmittance was relatively reduced much at the wavelength longer than 730 nm (periodicity of aligned arrays) because of diffraction of light occurred at the region of longer wavelength. On the other hand, the strong transmission efficiency at the wavelength less than 730 nm might be caused by the good matching of configuration and strong enhancement of the surface plasmon energy. For the nanobowls, surface plasmons (SPs) were excited at two Au/air interface (inside and outside the nanobowls), resulting in surface plasmon energy matching on the two sides of nanobowls.[44] Two dips were located at *ca.* 730 nm (refractive index of air is 1) and 1100 nm (refractive index of PVA film is about 1.5), respectively, when α and β were fixed at 0°. And they blue-shifted with the incidence angle α or β increased. This is an exact behavior observed when light couples with SPs in reflection gratings.[45,46] SPs are oscillations of surface charges at the metal interface and are excited when their momentum matches the momentum of the incident photon and the grating as follows:

$$k_{sp} = k_x + k_g$$

where k_{sp} is the surface plasmon wavevector, $k_x = (2\pi/\lambda)\sin\theta$ is the component of the incident photon's wavevector in the plane of the array (θ represents α or β, λ represents wavelength of incident light), and $k_g = 2\pi/na$ is the grating momentum wavevector for the aligned array (n means refractive index of dielectric, a means periodicity of the aligned array). In consequence, k_{sp} would increase with the increasing of α or β, leading to the transmission dip blue-shift. In addition, there was also a slight red-shift from *ca.* 730 nm in figure 4b which may be caused by periodic function in the direction perpendicular to Au nanobowls chains. However, the signals were overlapped with the blue-shift signals started from ca. 1100 nm when α increased lager enough.These preliminary results represent a motivation to carry on the study of surface plasmonic properties of this type of noble metal nanostructure. Eventually their application and fundamental scientific potential should be emphasized.

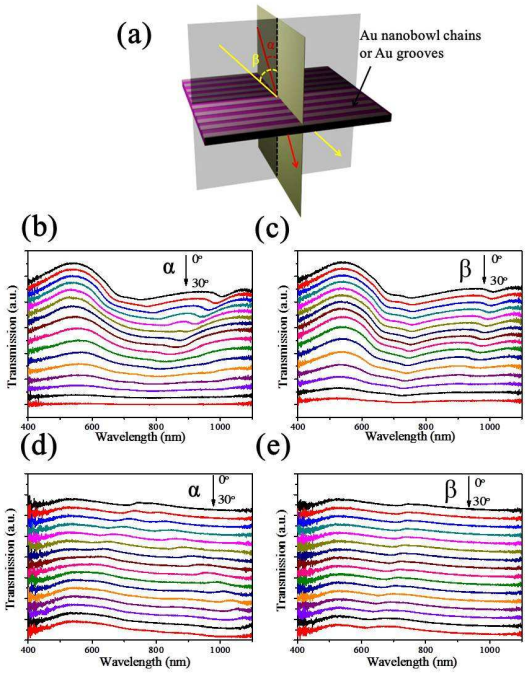

Fig. 4 (a) Schematic outline of the configuration of the incident light relative to the linear nanostructure. (b), (c) Angle-resolved transmission spectra of aligned Au nanobowl array. (d), (e) Angle-resolved transmission spectra of Au groove array.

For comparison, angle-resolved transmission spectra of DVD substrate coated with *ca.* 40 nm Au layer in the same condition were measured, as shown in figure 4d and e. When α and β were fixed at 0°, there was one dip at *ca.* 730 nm in the two spectra which was caused by SPR of Au grooves. While the dip blue-shifted with the angle α or β increased. In figure 5e, the shift of dip was much more notable than that in figure 5f, this was caused by different periodicity in different direction of the sample. Furthermore, there was no transmission enhancement at the wavelength less than 730 nm compared with aligned Au nanobowl array.

3.3 Optical grating with high reflectance

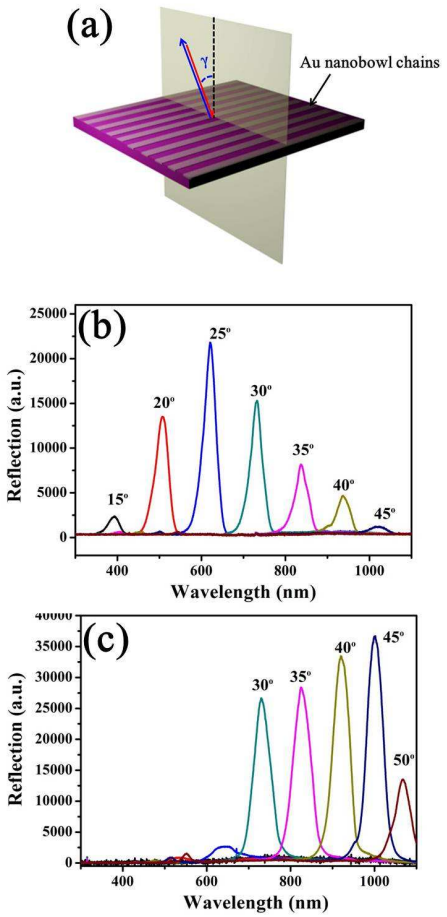

Fig. 5 (a) Schematic outline of the configuration of the incident light relative to the grooves on DVD substrate or the Au nanobowl linear nanostructure for measurements of reflectance spectra; (b) and (c) Reflectance spectra of DVD substrate and aligned Au nanobowl arrays.

DVD substrate with aligned grooves and aligned Au nanobowl arrays can be considered as gratings. We further investigated angle-resolved reflection spectra of both a DVD substrate with aligned grooves and aligned Au nanobowl arrays. Figure 5a schematically shows the orientation of the incident light relative to the grooves on DVD substrate or the Au nanobowl chains for measurements of reflection spectra. As can be seen, the prepared sample was fixed horizontally, and light source and detector were rotated at the same location simultaneously, so that backscattered light from the sample would be detected. The incident light was moving in the planar perpendicular to DVD grooves or Au nanobowl chains, and angle γ increased from 15° to 50°. The reflection spectra were recorded varying incidence angle of an interval of 5° for each measurement. In this way, the diffraction peak of 2-dementional patterns can be measured.[47] Figure 5b, 5c present angle-resolved reflection spectra of DVD substrate with aligned grooves and aligned Au nanobowl arrays, respectively. Some fascinating phenomena can be observed from two reflectance spectra. As can be seen in the two spectra, the peak appeared at specific angles when changed the incident light angle, and the peak continuously shifted to longer wavelength with the increasing of incident light angle. For DVD substrate, the peak intensity gradually increased when incident light angle increased from 15° to 25° and then decreased thereafter. This intensity change may be caused by the combined effect of the angular dependence of the irradiated area and the reflectivity of the substrate. For aligned Au nanobowl arrays, there was no obvious signal in the spectra when the incident light angle was less than 30°. However, peaks appeared when the incident light angle increased from 30° to 50°. This phenomenon might be caused by reasons as follow: when the incident angle was less than 30°, back-reflected light from the flat Au surface excited gap plasmons in the small gaps between the neighboring gold bowls, which were then adiabatically nanofocused in the gaps in the direction away from the surface. The gap plasmons subsequently dissipated their energy through style of ohmic losses, leading to the strong absorption. Therefore, the reflectance below 30° of incidence angle is quite low. When the angle of incidence increased large enough, the light eventually stopped being able to excite gap plasmons via back-reflection in this configuration, and lossy adiabatic nanofocusing no longer occurred. Therefore, the optical reflection dominated on top surface of the bowls[48]. After all, regarding to the peak intensity, the peaks in figure 5c were much stronger then these of figure 5b, which may be caused by two reasons as follow. On the one hand, the power in diffraction peak is related to the amplitude of the grating.[49] In this case, the depth of grooves on DVD substrate (*ca.* 100nm) and the height of Au nanobowls (*ca.* 400 nm) were the amplitudes. It is oobviously that the amplitude of aligned Au nanobowl arrays is greater than that of DVD substrate. On the other hand, the intensity of peak also directly depends on reflective index of samples. As we all know that the reflective index of Au is much bigger than that of polycarbonate (DVD substrate). As can be concluded that, aligned Au nanobowl arrays demonstrate much stronger reflectance than general gratings at certain wavelength region.

4. Conclusion

In conclusion, we develop a simple route with low cost to fabricate large-area aligned Au nanobowl arrays by combination of template-assisted self-assembly and colloids lithography. Notably, this structure with a high aspect ratio configuration and symmetry-reducing units is anisotropy in optical response, which was confirmed by angle-resolved transmission measurements. Such optical anisotropy is resulted by different LSPR mode along and across aligned Au nanobowl chains. Additionally, the aligned Au nanobowl arrays can be used as optical grating with higher reflectance. Owing to the special optical properties, this aligned Au nanobowl arrays have important applications in many fields of optical sensing, biological detection, and so on.

Acknowledgements

The authors acknowledge the financial support from the National Basic Research Program of China (Grant No. 2012CB932303), Recruitment Program of Global Experts (C), Natural Science Foundation of China (Grant Nos. 51371165), Cross-disciplinary Collaborative Teams Program in CAS, International Innovative Research Team in CAS.

Notes and references

1. T. Song, J. L. Xia, J. H. Lee, D. H. Lee, M. S. Kwon, J. M. Choi, J. Wu, S. K. Doo, H. Chang, W. Park, D. S. Zang, H. Kim, Y. G. Huang, K. C. Hwang, J. A. Rogers, U. Paik, *Nano Lett.*, 2010, **10**, 1710.
2. V. E. Ferry, M. A. Veerschuuren, H. B. T. Li, W. Verhagen, R. J. Walters, R. E. I. Schropp, H. A. Atwater, A. Polman, *Opt. Express*, 2010, **18**, 237.
3. J. W. Liu, J. Esssner, J. Li, *Chem. Mater.*, 2010, **22**, 5022.
4. W. B. Wei, K. Chen, G. L. Ge, *Adv. Mater.*, 2013, **25**, 3863.
5. X. X. Chen, H. M. Gong, S. W. Dai, D. Zhao, Y. Q. Yang, Q. Li, M. Qiu, *Opt. Lett.*, 2013, **38**(13), 2247.
6. L. Shao, Q. F. Ruan, R. B. Jiang, J. F. Wang, *Small*, 2014, **10**, 802.
7. A. B. D. Brown, C. G. Smith, A. R. Rennie, *Phys. Rev. E* 2000, **62**, 951.
8. H. M. Lee, Y. N. Kim, B. H. Kim, S. O. Kim, W. O. Cho, *Adv. Mater.*, 2008, **20**, 2094.
9. B. D. Terris, T. Thomson, *J. Phys. D: Appl. Phys.*, 2005, **38**, 199.
10. C. L. C. Smith, B. Desiatov, I. Goykmann, I. Fernandez-Cuesta, U. Levy, A. Kristensen, *Opt. Express*, 2012, **20**, 5696.
11. A. A. Tseng, *J. Micromech. Microeng.*, 2004, **14**, 15.
12. H. Bai, C. Du, A. J. Zhang, L. Li, *Angew. Chem. Int. Ed.*, 2013, **52**, 12240.
13. A. R. Tao, J. X. Huang, P. D. Yang, *Accounts Chem. Res.*, 2008, **41**, 1662.
14. Y. Li, G. T. Duan, G. Q. Liu, W. P. Cai, *Chem. Soc. Rev.*, 2013, **42**, 3614.
15. Y. Li, N. Koshizaki, W. P. Cai, *Coordin. Chem. Rev.*, 2011, **255**, 357.
16. Z. F. Dai, L. C. Jia, G. T. Duan, Y. Li, H. W. Zhang, J. J. Wang, J. L. Hu, W. P. Cai, *Chem. Eur. J.*, 2013, **19**, 13387.
17. D. Babonneau, S. Camelio, L. Simonot, F. Pailloux, P. Guérin, B. Lamongie, O. Lyon, *EPL*, 2011, **93**, 26005.
18. T. W. H. Oates, M. Ranjan, S. Facsko, H. Arwin, *Opt. Express*, 2011, **19**, 2014.
19. M. Ranjan, T. W. H. Oates, S. Facsko, W. Möller, *Opt. Lett.*, 2010, **35**, 2576.
20. R. Verre, K. Fleischer, O. Ualibek, I. V. Shvets, *Appl. Phys. Lett.*, 2012, **100**, 031102.
21. T. W. H. Oates, A. Keller, S. Facsko, A. Mücklich, *Plasmonics*, 2007, **2**, 47.
22. A. Toma, D. Chiappe, D. Massabo, C. Boragno, F. B. Mongeot, *Appl. Phys. Lett.*, 2008, **93**, 163104.
23. O. M. Liedke, B. Liedke, A. Keller, B. Hillebrands, A. Mucklich, S. Facsko, J. Fassbender, *Phys. Rev. B*, 2007, **75**, 220407.
24. M. Ranjan, S. Fascko, M. Fritzsche, S. Mukherjee, *Microelecton. Eng.*, 2013, **102**, 44.
25. M. Ranjan, *J. Nanopart. Res.*, 2013, **15**, 1908.
26. P. Albella, B. Garcia-Cueto. F. González, F. Moreno, P. C. Wu, T. H. Kim, A. Brown, Y. Yang, H. O. Everitt, G. Vidden, *Nano Lett.*, 2011, **11**, 3531.
27. M. A. Mahmoud, M. A. El-sayed, *J. Am. Chem. Soc.*, 2010, **132**, 12704.
28. H. Q. Wang, L. C. Jia, L. Li, Z. Swiatkowska-Warkocka, K. Kawaguchi, A. Pyatenko, N. Koshizaki, *J. Mater. Chem. A*, 2013, **1**, 692.
29. M. Gkikas, J. Timonen, J. Ruokolainen, P. Alexandridis, H. Iatrou, *J. Polym. Sci. Pol. Chem.*, 2013, **51**, 1448.
30. P.Y. Lim, R.S. Liu, P.L. She, C.F. Hung, H.C. Shih, *Chem. Phys. Lett.*, 2006, **420**, 304.
31. Y. Li, C. C. Li, S. O. Cho, G. T. Duan, W. P. Cai, *Langmuir*, 2007, **23**, 9802.
32. J. Ye, P. V. Dorpe, W. V. Roy, G. Borghs, G. Maes, *Langmuir*, 2009, **25**, 1822.
33. C. T. Cooper, M. Rodriguez, S. Blair, J. S. Shumaker-Parry, *J. Phys. Chem. C*, 2014, **118**, 1167.
34. C. C. Kei, T. H. Chen, C. M. Chang, C. Y. Su, C. T. Lee, C. N. Hsiao, S. C. Chang, T. P. Perng, *Chem. Mater.*, 2007, **19**, 5833.
35. M. G. Banaee, K. B. Crozier, *Opt. Lett.*, 2010, **35**, 760.
36. K. L. Hobbs, P. R. Larson, G. D. Lian, J. C. Keay, M. B. Johnson, *Nano Lett.*, 2004, **4**, 167.
37. C. Charnay, A. Lee, S. Man, C. E. Moran, C. Radloff, R. K. Bradley, N. Halas, *J. Phys. Chem. B*, 2003, **107**, 7327.
38. M. Cortie, M. Ford, *Nanotechnology*, 2007, **18**, 235704.
39. J. Ye, P. V. Dorpe, W. V. Roy, K. Lodewijks, I. D. Vlaminck, G. Maes, G. Borghs, *J. Phys. Chem. C*, 2009,**113**, 3110.
40. J. Ye, P. V. Dorpe, W. V. Roy, G. Borghs, G. Maes, *Langmuir*, 2009, **25**, 1822.
41. Y. D. Yin, Y. Lu, B. Gates, Y. N. Xia, *J. Am. Chem. Soc.*, 2001,**123**, 8718.
42. Y. D. Yin, Y. Lu, Y. N. Xia, *J. Am. Chem. Soc.*, 2001,**123**, 771.
43. Y. N. Xia, Y. D. Yin, Y. Lu, J. McLellan, *Adv. Funct. Mater.*, 2003, **13**, 907.
44. B. Ai, Y. Yu, H Mohwald, G. Zhang, *Nanotech.*, 2013, **24**, 035303.
45. R. H. Ritchie, E. T. Arakawa, J. J. Cowan, R. N. Hamm, *Phys. Rev. Lett.*, 1968, **21**, 1530.
46. T. W. Ebbesen, H. J. Lezec, H. F. Ghaemi, T. Thio, P. A. Wolff, *Nature*, 1998, **391**, 667.
47. T. Kanai, T. Sawada, K. Kitamura, *Langmuir*, 2003, **19**, 1984.
48. T. Søndergaard, S. M. Novikov, T. Holmgaard, R. L. Eriksen, J. Beermann, Z. Han, K. Pedersen, S. I. Bozhevolnyi, *Nat. Commun.*, 2012, **3**, 969.
49. E. Marx, T. A. Germer, T. V. Vorburger, B. C. Park, *Appl. Optics*, 2000, **39**, 4473.

Graphical Table of Contents

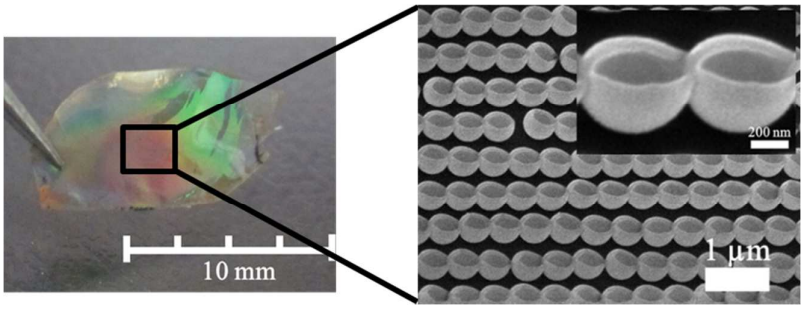

Aligned Au nanobowl arrays on a flexible film with specific optical properties were obtained by combination template-assisted self-assembly with colloidal lithography.